Program Digest, 2019 IEEE International Ultrasonics Symposium (IUS)
Glasgow, Scotland, October 6-9, 2019

Non-rigid Motion Correction for Ultrasound Localization Microscopy of the Liver *in vivo*

Yayu Hao[1], Qin Wang[2], Yi Yang[1], Zhi Liu[1], Qiong He[1], Lai Wei[3], Jianwen Luo[1,*]
[1]Department of Biomedical Engineering, Tsinghua University, Beijing, China
[2]Peking University First Hospital, Beijing, China
[3]Hepatopancreatobilary Center, Beijing Tsinghua Changgung Hospital, Tsinghua University, Beijing, China
[*]Email: luo_jianwen@tsinghua.edu.cn

***Abstract*—Chronic liver diseases (CLDs) are a major killer of humans, and more than 1 billion people suffer from CLDs worldwide, which are likely to develop significant liver fibrosis (LF) and even cirrhosis. However, current noninvasive diagnostic methods for liver diseases are insensitive to early lesions, so accurate assessment of LF at early stage is very important for the treatment arrangement and fibrosis reversal before cirrhosis. Ultrasound localization microscopy (ULM) with contrast microbubbles (MBs) have been proposed by several groups and may have potential in evaluating LF at early stage. Unfortunately, breathing and heart beating can introduce motion artifacts in liver ULM, which brings the challenge for LF evaluation with ULM. Recently, rigid motion correction (MoCo) has been proposed to improve the performance of ULM of the brain and kidney. Considering typical non-rigid motion in the liver, the performance of rigid MoCo may be limited. Therefore, we propose a non-rigid MoCo method based on speckle tracking to improve the performance of liver ULM more effectively. Results of *in vivo* experiments indicate that ULM with non-rigid MoCo obtains better resolution and more continuous microvessels (MVs) than rigid MoCo.**

Keywords—Liver fibrosis, motion estimation, motion correction, non-rigid motion, speckle tracking, ultrasound localization microscopy

I. Introduction

More than 1 billion people in the world suffer from chronic liver diseases (CLDs) and about one third of them are likely to develop significant fibrosis and even cirrhosis [1]. In China, CLDs affect about 400 million people, and there are at least 100 million patients with significant liver fibrosis (LF) [2]. Cirrhosis has a very high mortality and is generally treated with liver transplant, while LF is the early stage of cirrhosis. Fortunately, LF is reversible with appropriate treatment. Therefore, accurate assessment of LF is very important for the treatment arrangement and fibrosis reversal before cirrhosis. Liver biopsy has been regarded as the gold standard for LF staging. However, the limitations of invasiveness and poor repeatability make it not suitable for routine screening [3]. Biomarkers, such as aspartate transaminase-to-platelet ratio index (APRI) and fibrosis index based on four factors (FIB-4), are also used to assess LF, but their diagnostic performance remains controversial in some LF patients [4]. In recent years, several ultrasound elastography methods have been developed to stage LF noninvasively [5-7], including transient elastography, two-dimensional (2D) shear wave elastography and other methods, which generally achieve better accuracy of LF evaluation than conventional ultrasound imaging. Nevertheless, due to the unapparent change of elasticity in the early stage of LF, ultrasound elastography may be not a sensitive tool to accurate assessment of LF in early stage [8].

ULM is a novel ultrasound imaging method with outstanding resolution for microvessel (MV) imaging and reveals a huge potential for clinical application [9, 10]. ULM would be helpful for understanding the pathogenesis of LF, especially at early stage. Unfortunately, the irregular geometry of the liver and its anatomical location adjacent to the heart make it susceptible to breathing and heart beating. The complexity of breathing and heart beating makes liver movement non-rigid and large, which can introduce evident artifacts in liver ULM. Recently, several rigid motion correction (MoCo) methods have been proposed to improve the performance of ULM of the brain [11], kidney [12] and other organs. However, their performances may be ineffective in ULM of the liver with non-rigid motion. The objective of this study is to develop a non-rigid MoCo method for ULM of the liver *in vivo*.

Speckle tracking is typically used for motion estimation and has been widely used in various ultrasound imaging modalities, including blood flow imaging [13], elastography [14], temperature imaging [15] and phase-aberration correction [16]. In this study, we employed a 2D normalized cross-correlation (NCC) based speckle tracking technique to estimate liver displacements, which were subsequently used for motion correction (MoCo) of the location of MB centers. This technique was tested in a mouse liver *in vivo*.

II. Methods

A. Animal Preparation and Data Acquisition

Approved by the Medical Ethics Committee of Peking University First Hospital (Beijing, China), a normal c57BL/6 mouse at the age of 6 weeks was examined. A Verasonics Vantage system (Verasonics, Redmond, WA, USA) equipped with an L15-Xtech linear array (Vermon, Tours, France) was utilized for data acquisition. 6,000 frames of radiofrequency (RF) channel data of the mouse liver in the sagittal plane were acquired with plane wave imaging. 5 angles from -12° to 12°, with a step of 6° and a pulse repetition rate of 2,000 Hz were used for coherent compounding. And the effective frame rate after compounding was 400 Hz.

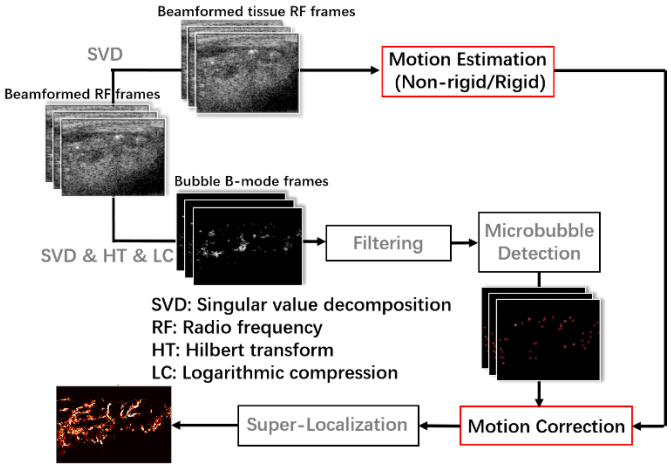

Fig. 1. Processing chain of ULM with non-rigid MoCo.

B. ULM Algorithm with MoCo

The overall processing chain of ULM with non-rigid MoCo is shown in Fig. 1. Delay-and-sum (DAS) beamforming was first performed on the channel data. Singular value decomposition (SVD) based spatiotemporal filtering [17] was applied to extract the MBs from the surrounding liver tissues. Thereafter, the motion caused by breathing and heart beating was then estimated from the beamformed RF data by the proposed non-rigid MoCo method (detailed in Section II-C), which was used to compensate the locations of MB centers in the following steps. The singular value order of SVD-based filtering was selected empirically. The results before and after SVD-based filtering are shown in Figs. 2(a) and 2(b), respectively. After a thresholding operation to reduce the noise and an interpolation operation in the lateral direction, the individual MBs were localized by 2D Gaussian fitting [12]. The method to detect individual MBs was the same as that used in our previous work [18] and the result of the first frame is shown in Fig. 2(c). The regions that were too large or too small in size, too weak in intensity or not almost circular were then discarded. The remaining regions were taken as individual MBs, and localized by 2D Gaussian fitting. Finally, a localization density map of the liver with super-resolution was obtained by accumulating all the locations of MBs extracted from all the images, accompanying with motion compensation in the meanwhile. The profiles of two MVs (detailed in Section III-B) were used to evaluate the liver ULM resolution. For comparison, rigid MoCo was also implemented.

C. Displacement Estimation

As for non-rigid MoCo in ULM of the liver, the axial and lateral displacements were estimated from the RF frames of the liver after SVD filtering using a 2D NCC based speckle tracking algorithm. A 2D kernel (2 mm × 2 mm) with an axial overlap of 94% was used. Axial cosine interpolation was used to estimate subsample axial displacements while lateral interpolation on both the RF signals and cross-correlation function was used to estimate subsample lateral displacements [19].

The detailed procedure is describing as the following. Firstly, the first frame was taken as the reference frame and the second frame was taken as the comparison frame. Then, 2D NCC based speckle tracking was performed between the reference and comparison frames; the axial and lateral displacements, as well as the correlation coefficients between kernels on the reference and comparison frames, were obtained. Next, we manually selected the rough liver region on the first frame. Thereafter, the average correlation coefficient in the selected liver region was calculated. A strategy of dynamic reference frame selection was implemented to ensure the reliability of displacement estimation. When the average correlation coefficient in the liver region was lower than a threshold (i.e., 0.7), the reference frame was changed to the previous frame of the current comparison frame. Due to the continuity of liver motion, the average correlation coefficient in the liver region between the new reference frame and the comparison frame was generally higher than the threshold. After all the frames were processed, the accumulated displacements between the first frame and all the other frames were obtained. . Furthermore, the estimated displacements were interpolated to have the size same as the ULM image. Finally, the locations of MB centers were compensated with the interpolated displacements frame by frame.

Differently from non-rigid MoCo, rigid MoCo only needs to estimate the global displacements in both axial and lateral directions rather than the displacement distribution. In this study, a high-echogenicity point was manually selected in the middle on the first frame of B-mode image (i.e., p1 in Fig. 2(a)). A 2D kernel (2 mm × 2 mm) centered at this point was used to track the displacements. Dynamic reference frame selection was also used and the kernel was updated according to the estimated displacements when the reference frame was changed. Finally, the displacements were accumulated and used for rigid MoCo.

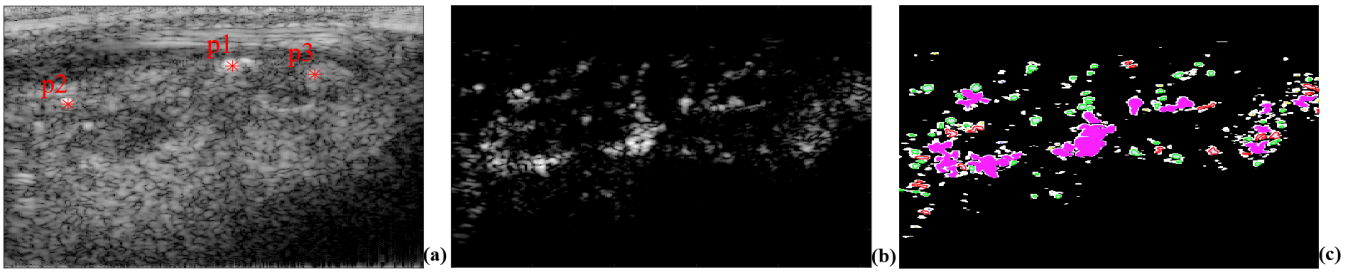

Fig. 2. Procedure of individual MB detection. (a) B-mode image of the frame before SVD filtering. (b) B-mode image of the frame after SVD filtering. (c) Detection of individual MBs. Blue: weak noise; pink: too large size; yellow: too small size; white with red margin: overlapped MBs; white with green margin: individual MBs to be localized.

III. Results

A. Non-rigid Displacement Estimation

Fig. 3 illustrates the lateral and axial displacement curves of three typical positions in high-echogenicity regions (labeled in Fig. 2(a)). The average periods of motion in the lateral and axial directions are the same and are about 792 ms. The motion rightward or upward is defined as positive motion. As shown in Fig. 3(a), the peak lateral displacements increase as the position changes from the left to right. And the average peak lateral displacements at p2, p1, p3 are -0.515, -0.649, -0.749 mm, respectively, with a difference between each two being more than 100 μm. In Fig. 3(b), the difference of axial displacement curves at different positions is larger with the opposite motions shown. The average peak axial displacements at p2, p1, p3 are 0.028, -0.034, -0.057 mm, respectively, with a difference between p2 and p3 being about 85 μm. From comparison between Figs. 4(a) and (b), it is found that lateral displacements of the liver are one order of magnitude larger than the axial displacements.

B. ULM of Liver In Vivo

As shown in Fig. 4(a), the ULM image without MoCo has evident motion artifacts in the areas pointed by the red arrows, which make the MVs blurry. Both rigid and non-rigid MoCo can improve the performance of the liver ULM and obtain better spatial resolution (Fig. 4(b) and 4(c)). The transverse profiles of ULM image are obtained across the MVs at two different locations (green curves in Figs. 4(a)-(c)). The full width at half maximum (FWHM) obtained from the profiles is calculated. For each method, the resolution of ULM is evaluated by the FWHM of MV. The profiles and results of FWHMs are shown in Figs. 4(e)-(f). In Fig. 4(e), rigid and non-rigid MoCo obtain similar FWHMs for the single MV. The FWHMs of the MV are 173 and 168 μm for rigid and non-rigid MoCo, respectively. In Fig. 4(f), non-rigid MoCo obtains smaller FWHMs than rigid MoCo in all the three MVs. The FWHMs of the three MVs are 112, 169, 159 μm for rigid MoCo, and are 105, 132, 144 μm for non-rigid MoCo, respectively. Furthermore, non-rigid MoCo obtains more continuous MVs than rigid MoCo (white arrow in Figs. 5(d)).

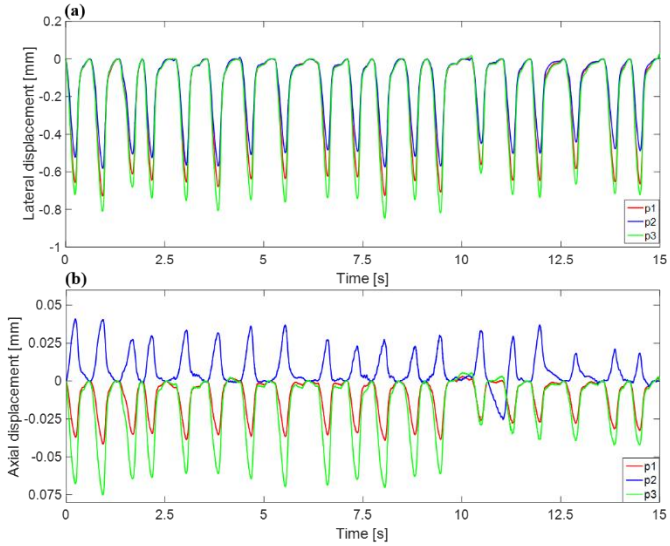

Fig. 3. (a) Lateral and (b) axial displacement curves at the three positions indicated in Fig. 2(a).

IV. Discussion

In this study, we demonstrated that the motion of liver is typically non-rigid and the complex motion can introduce the evident artifacts in ULM of the liver, which may also affect the assessment of LF. To mitigate this problem, a non-rigid MoCo method was developed to compensate for the motion of liver in vivo. Compared to rigid MoCo, non-rigid MoCo improved the performance of liver ULM more effectively.

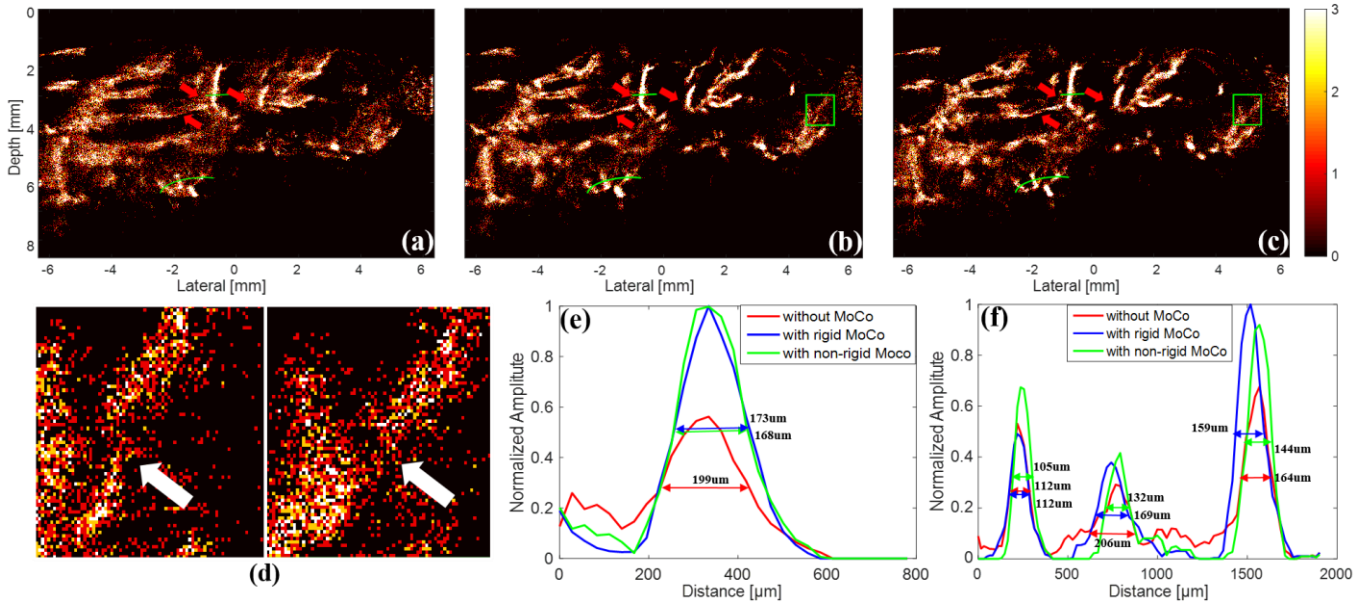

Fig. 4. ULM images of the liver in the sagittal plane (a) without MoCo, (b) with rigid MoCo and (c) with non-rigid MoCo, respectively. (d) The enlarged view of the green rectangles in (b) and (c). Normalized amplitudes along the green curves in (a)-(c) across the microvessels (e) on the upper middle and (f) bottom left, respectively.

A. Analysis of Results

As described in Section III-A, both lateral and axial displacements demonstrate the non-rigid feature of the liver motion. According to the displacements at different points in the liver, non-rigid MoCo is necessary in liver ULM, because an error of tens of micrometers is large enough to affect the MV evaluation in ULM.

As shown in Fig. 4(f), non-rigid MoCo achieves better resolution than rigid MoCo for all the three MVs, which demonstrates the advantages of non-rigid MoCo over rigid MoCo. However, non-rigid and rigid MoCo achieve similar FWHMs in Fig. 4(e). It may be explained by the kernel selection for rigid MoCo. The kernel was centered at p1 (Fig. 2(a)), and the single MV (green line in Figs. 5(a)-(c)) is adjacent to p1. In this area, the estimated displacements used in rigid MoCo are similar to those used in non-rigid MoCo. As a result, non-rigid and rigid MoCo perform similarly FWHMs in Fig. 4(e).

B. Limitation of Non-rigid MoCo

It should be noted that non-rigid MoCo is a time-consuming task. Several hours are needed for processing 6,000 frames with 256 × 700 pixels by non-rigid MoCo, while rigid MoCo only needs about ten minutes. Actually, the motions within the entire field of view were estimated for each frame in this study. Some accelerating methods (e.g., calculating the displacements only at the MB centers on each frame) may be implemented to reduce the processing time.

C. Outlook of Liver ULM with Non-rigid MoCo

In this study, ultrafast plane wave imaging was utilized to track the rapid flowing of MBs in the mouse liver, which can further provide the information of blood flow velocity and direction. Together with the structural information of MVs, the information of blood flow may be used to stage LF in the future.

CONCLUSIONS

In this study, we developed a non-rigid MoCo method based on 2D NCC algorithm for liver ULM and demonstrated that the non-rigid MoCo method can improve the performance more effectively for ULM of the mouse liver *in vivo* than the rigid MoCo method. ULM with non-rigid MoCo may be applied to evaluate LF in early stage for diagnosis and treatment of CLDs.

ACKNOWLEDGMENTS

The authors thank Dr. Yinran Chen in our laboratory for providing the accelerated beamforming program

REFERENCES

[1] M. Pinzani, K. Rombouts, and S. Colagrande, "Fibrosis in chronic liver diseases: diagnosis and management," Journal of Hepatology, vol. 42, pp. S22-S36, 2005.

[2] W. Fu-Sheng, F. Jian-Gao, Z. Zheng, G. Bin, and W. Hong-Yang, "The global burden of liver disease: the major impact of China," Hepatology, vol. 60, pp. 2099-2108, 2015.

[3] S. M. Martínez, C. Gonzalo, N. Miquel, and F. Xavier, "Noninvasive assessment of liver fibrosis," Hepatology, vol. 53, pp. 325-335, 2011.

[4] W. R. Kim, T. Berg, T. Asselah, R. Flisiak, S. Fung, S. C. Gordon, et al., "Evaluation of APRI and FIB-4 scoring systems for non-invasive assessment of hepatic fibrosis in chronic hepatitis B patients," Journal of Hepatology, vol. 64, pp. 773-780, 2016.

[5] N. A. Terrault, A. S. Lok, B. J. Mcmahon, K. M. Chang, J. P. Hwang, M. M. Jonas, et al., "Update on prevention, diagnosis, and treatment and of chronic hepatitis B: AASLD 2018 hepatitis B guidance," Hepatology, vol. 67, 2018.

[6] L. European Assoc Study, "EASL 2017 Clinical practice guidelines on the management of hepatitis B virus infection," Journal of Hepatology, vol. 67, pp. 370-398, 2017.

[7] C. F. Dietrich, J. Bamber, A. Berzigotti, S. Bota, V. Cantisani, L. Castera, et al., "EFSUMB guidelines and recommendations on the clinical use of liver ultrasound elastography, update 2017 (Short Version)," Ultraschall in Der Medizin, vol. 38, pp. 377-394, 2017.

[8] F. Giovanna, T. Carmine, D. B. Barbara, Z. Mabel, F. Gaetano, and F. Carlo, "Accuracy of real-time shear wave elastography for assessing liver fibrosis in chronic hepatitis C: a pilot study," Hepatology, vol. 56, pp. 2125-2133, 2012.

[9] E. Claudia, P. Juliette, P. Sophie, D. Yann, L. Zsolt, C. Olivier, et al., "Ultrafast ultrasound localization microscopy for deep super-resolution vascular imaging," Nature, vol. 527, pp. 499-502, 2015.

[10] S. Dencks, M. Piepenbrock, T. Opacic, B. Krauspe, E. Stickeler, F. Kiessling, et al., "Clinical pilot application of super-resolution US imaging in breast cancer," Ieee Transactions on Ultrasonics Ferroelectrics and Frequency Control, vol. 66, pp. 517-526, 2019.

[11] V. Hingot, C. Errico, M. Tanter, and O. Couture, "Subwavelength motion-correction for ultrafast ultrasound localization microscopy," Ultrasonics, vol. 77, pp. 17-21, 2017.

[12] P. Song, J. D. Trzasko, A. Manduca, R. Huang, R. Kadirvel, D. F. Kallmes, et al., "Improved super-resolution ultrasound microvessel imaging with spatiotemporal nonlocal means filtering and bipartite graph-based microbubble tracking," IEEE Transactions on Ultrasonics Ferroelectrics & Frequency Control, vol. PP, pp. 1-1, 2018.

[13] G. E. Trahey, J. W. Allison, and O. T. Ramm, Von, "Angle independent ultrasonic detection of blood flow," Biomedical Engineering IEEE Transactions on, vol. BME-34, pp. 965-967, 1987.

[14] J. Ophir, S. K. Alam, B. S. Garra, F. Kallel, E. E. Konofagou, T. Krouskop, et al., "Elastography: imaging the elastic properties of soft tissues with ultrasound," Journal of Medical Ultrasonics, vol. 29, p. 155, 2002.

[15] T. Varghese, J. A. Zagzebski, and F. T. L. Jr, "Elastographic imaging of thermal lesions in the liver in vivo following radiofrequency ablation: preliminary results," Ultrasound in Medicine & Biology, vol. 28, pp. 1467-1473, 2002.

[16] G. C. Ng, S. S. Worrell, P. D. Freiburger, and G. E. Trahey, "A comparative-evaluation of several algorithms for phase aberration correction," Ieee Transactions on Ultrasonics Ferroelectrics and Frequency Control, vol. 41, pp. 631-643, 1994.

[17] C. Demené, T. Deffieux, M. Pernot, B. F. Osmanski, V. Biran, J. L. Gennisson, et al., "Spatiotemporal clutter filtering of ultrafast ultrasound data highly increases doppler and fUltrasound sensitivity," IEEE Transactions on Medical Imaging, vol. 34, pp. 2271-2285, 2015.

[18] Y. Yang, Q. He, H. Zhang, L. Qiu, L. Qian, F.-F. Lee, et al., "Assessment of diabetic kidney disease using ultrasound localization microscopy: an in vivo feasibility study in rats," Proceedings of IEEE International Ultrasonics Symposium, pp. 1-4, 2018.

[19] Z. Liu, C. Huang, and J. Luo, "A systematic investigation of lateral estimation using various interpolation approaches in conventional ultrasound imaging," IEEE Transactions on Ultrasonics Ferroelectrics & Frequency Control, vol. 64, pp. 1149-1160, 2017.